Available online at www.sciencedirect.com
ScienceDirect
Solid-State Electronics 50 (2006) 1677–1681
SOLID-STATE ELECTRONICS
www.elsevier.com/locate/sse

ICP-induced defects in GaN characterized by capacitance analysis

Wen-How Lan [a,*], Kuo-Chin Huang [b], Kai Feng Huang [b]

[a] Department of Electrical Engineering, National University of Kaohsiung, Kaohsiung 811, Taiwan, ROC
[b] Department of Electrophysics, National Chiao Tung University, Hsinchu 300, Taiwan, ROC

Received 18 May 2005; received in revised form 23 September 2006; accepted 5 October 2006

The review of this paper was arranged by C. Tu

Abstract

The defects induced by inductively coupled plasma reactive ion etching (ICP-RIE) on a Si-doped gallium nitride (GaN:Si) surface have been analyzed. According to the capacitance analysis, the interfacial states density after the ICP-etching process may be higher than 5.4×10^{12} eV^{-1} cm^{-2}, compared to around 1.5×10^{11} eV^{-1} cm^{-2} of non-ICP-treated samples. After the ICP-etching process, three kinds of interfacial states density are observed and characterized at different annealing parameters. After the annealing process, the ICP-induced defects could be reduced more than one order of magnitude in both N_2 and H_2 ambient. The H_2 ambient shows a better behavior in removing ICP-induced defects at a temperature around 500 °C, and the interfacial states density around 2.2×10^{11} eV^{-1} cm^{-2}can be achieved. At a temperature higher than 600 °C, the N_2 ambient provides a much more stable interfacial states behavior than the H_2 ambient.

Keywords: GaN; ICP; Current transport mechanism; Schottky diodes

1. Introduction

Gallium nitride (GaN) has been intensively studied because of its potentials for high-temperature and high-power electronic device applications [1–4]. Since GaN is quite hard to etch, inductively coupled plasma reactive ion etching (ICP-RIE) method is generally applied. Several groups have carried out studies of defects induced by the ICP-etching process [5–9]. It is known that ion bombardment in the ICP-etching process may cause material and/or device damage. The leakage current and breakdown voltage [10,11] of devices in the reverse bias region are generally used to characterize ICP-etching GaN samples. On the other hand, Lee et al. [12] have reported that a high leakage current for an ICP-etched GaN Schottky diode can be observed. With the following rapid thermal annealing process, the leakage current decrease with the annealing temperatures increase. Cheung et al. [13] have performed optical characterization of GaN on RIE-induced effects. Achouche et al. [14] has reported electrical characterization of InAlAs with RIE-induced damage. Many groups have discussed ICP-RIE-induced defect of GaN or other compound semiconductors. However, the interfacial state density of a GaN Schottky contact with ICP-induced defects have not been characterized by capacitance–frequency (*C–f*) measurements in these reports.

In this work, we study thermal-treated effects of GaN Schottky contact after ICP-etching. The thermal-treated effects are analyzed and the defect density is determined by capacitance–frequency (*C–f*) measurements over the frequency range (100 Hz–1 MHz) at room temperature. We find that the defects caused by the ICP-etching process can be partially eliminated by the annealing process. Besides the annealing ambient temperature is also important to eliminate these defects.

* Corresponding author. Tel.: +886 7 5919 437; fax: +886 7 5919 374.
E-mail address: whlan@nuk.edu.tw (W.-H. Lan).

0038-1101/$ - see front matter © 2006 Elsevier Ltd. All rights reserved.
doi:10.1016/j.sse.2006.10.005

2. Experiment

In this experiment, samples of Si-doped GaN epitaxial layers were grown by metal-organic chemical vapor deposition (MOCVD). The structure of the samples consists of a 2-μm-thick n-type GaN layer followed by a 2-μm-thick undoped GaN layer on a c-face sapphire substrate. The effective concentration was approximately $2\times10^{17}\,\mathrm{cm}^{-3}$ and the mobility was $450\,\mathrm{cm}^2$/V-s. The ohmic contacts were processed by thermal evaporation of Cr/Al/Cr/Au (150 Å/3000 Å/150 Å/3000 Å) and subsequent annealing at 600 °C for 20 min in N_2 ambient. The specific contact resistance (ρ_c) was around $1.2\times10^{-3}\,\Omega\,\mathrm{cm}^2$. Then, samples were exposed to ICP-RIE with Cl_2/Ar (30 sccm/10 sccm) gases. The pressure was 3 mTorr and the ICP power was 500 W. After the ICP-etching process, certain damages were expected in GaN. This was followed by the annealing process at different temperatures in N_2 or H_2 ambient to remove the ion damage. After different annealing conditions listed in Table 1, the samples were chemically treated by a $HCl:H_2O$(1:1) solution for 3 min, followed by Ni/Au (1000 Å/3000 Å) Schottky contact formation by photolithography. The contact area was $6\times10^{-4}\,\mathrm{cm}^2$. The capacitance and conductance measurements were performed with a Hewlett–Packard 4284 analyzer at room temperature. The junction capacitance of the Schottky contact was derived from the series resistance correction of the measured capacitance and conductance [15,16].

3. Results and discussion

With device capacitance and conductance measurement, the junction capacitance (C) is calculated according to the series resistance correction from the relation [17–20]

$$C = C_M/[(1-R_s\cdot G_M)^2+(2\pi\cdot f\cdot R_s\cdot C_M)^2], \quad (1)$$

where C_M and G_M are the measured device capacitance and conductance with simplified parallel equivalent circuit of a Schottky type contact, respectively, R_s is the series resistance, and f is the frequency.

For a Schottky contact with interfacial states, the junction capacitance, C, is the sum of the space charge capacitance, C_{sc}, and the interfacial states capacitance, C_p. The interfacial states capacitance C_p is then obtained from [21,22]

$$C_p = C - C_{sc}, \quad (2)$$

The space charge capacitance, C_{sc}, can be obtained by extrapolating the linear portion of the high-frequency (1 MHz) C^{-2}–V plot under reverse bias [20]. Fig. 1 shows the Schottky contact interfacial states capacitance for an as-grown n-GaN sample (R1) and as-ICP-etched sample (R2). The frequency dispersion in the interfacial states can be observed clearly. The interfacial states capacitance, which depends on the interfacial states density N_{ss} with a relaxation time τ, is given by [19–22]

$$C_p = qAN_{ss}\mathrm{arc\,tan}(\omega\tau)/\omega\tau, \quad (3)$$

where q is the electron charge, A is the contact area and ω ($=2\pi\cdot f$) is the angular frequency. According to Eq. (3), there is one plateau region in the frequency relation with a certain relaxation time. Singh [19] has reported Schottky diodes with different surface treated on the n-type CdF2:YF3 semiconductor, and defined the interfacial states density with fast and slow states by capacitance–frequency (C–f) methods. On the other hand, the numerical results of theoretical simulation of GaN Schottky diodes with different frequency regions are analyzed by Schmeits et al. [16]. Yet, in Fig. 1, the data manifest two plateau regions in the frequency range around 100 Hz–2 KHz and 100 KHz–300 KHz, respectively. There may be also different types of states in the semiconductor. This interfacial states capacitance can be considered to be the overall effect of different kinds of interfacial centers [16,23–25]. We can do the best fitting procedure in different frequency ranges [19] to distinguish these states. For each interfacial center, the interfacial states capacitance can be written as

$$C_{p\text{-}i} = C_p - C_{p\text{-}i\text{-}0}, \quad (4)$$

where i represent the i-type interfacial states (i = MF, HF) [16]. $C_{p\text{-}i\text{-}0}$ is the height of the plateaus region in the C_p-frequency relation. The dotted curves represent the fitting results of the experimental data in Fig. 1. In the frequency range 100 Hz to 2 KHz, the attractive MF-type interface states density $N_{ss\text{-}MF}$ of as-grown samples is $5.0\times10^{10}\,\mathrm{eV}^{-1}\,\mathrm{cm}^{-2}$. In the frequency range from 100 KHz to 1 MHz, the associated HF-type interfacial states density $N_{ss\text{-}HF}$ is $1.0\times10^{11}\,\mathrm{eV}^{-1}\,\mathrm{cm}^{-2}$. The relaxation time is 1.9×10^{-5} s and 2.7×10^{-7} s, respectively, as listed in Table 1. According to the work of Schmeits et al. [16], a single substitutional atom may act simulta-

Table 1
Summary of the interfacial states characteristics of samples with different treatments

Samples	$N_{ss\text{-}LF}$ ($\mathrm{eV}^{-1}\,\mathrm{cm}^{-2}$)	τ(s)	$N_{ss\text{-}MF}$	τ(s)	$N_{ss\text{-}HF}$ ($\mathrm{eV}^{-1}\,\mathrm{cm}^{-2}$)	τ(s)
As-grown	–	–	5.0×10^{10}	1.9×10^{-5}	1.0×10^{11}	2.7×10^{-7}
As-ICP-etched	4.3×10^{12}	1.0×10^{-3}	8.2×10^{11}	4.0×10^{-5}	2.4×10^{11}	3.2×10^{-7}
N_2 400	3.4×10^{12}	2.6×10^{-3}	2.6×10^{11}	6.5×10^{-5}	1.3×10^{11}	2.7×10^{-7}
N_2 500	1.9×10^{11}	2.0×10^{-3}	1.1×10^{11}	3.5×10^{-5}	6.0×10^{10}	2.7×10^{-7}
N_2 600	3.0×10^{10}	1.5×10^{-4}	5.8×10^{10}	2.4×10^{-5}	1.3×10^{11}	2.3×10^{-7}
H_2 400	2.8×10^{11}	1.0×10^{-3}	2.5×10^{11}	7.1×10^{-5}	4.8×10^{11}	2.7×10^{-7}
H_2 500	5.0×10^{10}	6.0×10^{-4}	4.2×10^{10}	4.0×10^{-5}	1.3×10^{11}	2.7×10^{-7}
H_2 600	1.1×10^{12}	5.8×10^{-4}	6.8×10^{10}	1.0×10^{-5}	1.6×10^{11}	2.7×10^{-7}

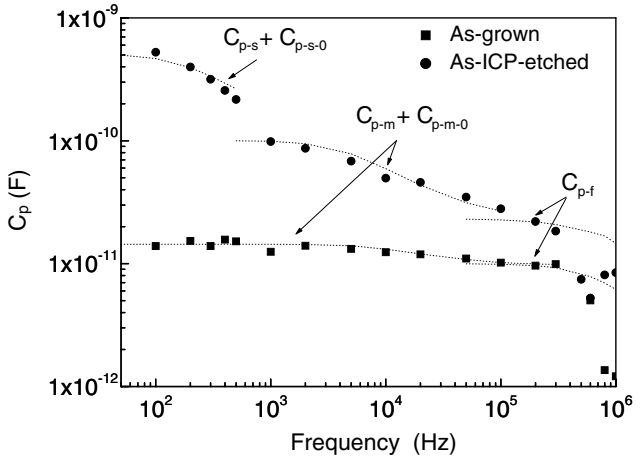

Fig. 1. Frequency dependence of the interfacial states capacitance of as-grown sample and as-ICP-etched sample. The dot curve represents the fitting result of the experiment data.

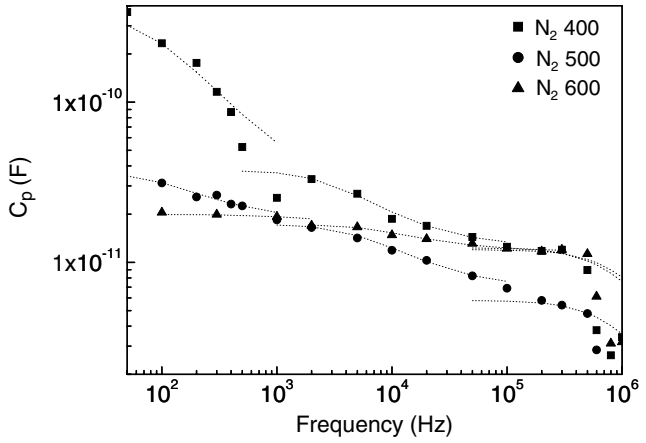

Fig. 2. Frequency dependence of C_p for the ICP-etched *n*-GaN sample after thermal annealing at 400 °C, 500 °C and 600 °C in N_2 ambient. The dot curves represent the fitting results of the experiment data.

neously as dopant and impurity, and two transition frequencies can be expected in theoretical calculations. The two transition frequencies in our sample may come from one impurity atom such as Si and/or other impurity and/or defect state. A detailed study is necessary to investigate the origin of these states in these samples.

For a sample after the ICP-etching process (R2), the results of the C_p vs. frequency are also shown in Fig. 1. Comparing to as-grown samples (R1), there are two plateau regions, indicative of some different types of interfacial centers of the GaN after ICP-etching process. Compared to the as-grown sample (R1), the ICP-etched sample (R2) may have a new interfacial state with low transition frequency around 300 Hz. Therefore, we assume that there are three kinds of interfacial states $N_{ss\text{-}LF}$, $N_{ss\text{-}MF}$ and $N_{ss\text{-}HF}$ with interfacial states capacitances $C_{p\text{-}LF}$, $C_{p\text{-}MF}$ and $C_{p\text{-}HF}$ respectively in the frequency range from 100 Hz to 1 KHz, 1 KHz to 100 KHz and 100 KHz to 1 MHz, respectively. We fit the C_p-frequency for each range by Eq. (4) with i = LF,MF,HF. The curves in this figure are the fitting results for each interfacial states capacitance. The fitting results are listed in Table 1. There are different types of interfacial states in the GaN sample after ICP-etching. In this case, the LF-type of interfacial states ($N_{ss\text{-}LF}$) becomes dominant, and the density is around $4.3 \times 10^{12}\,eV^{-1}\,cm^{-2}$ in our sample (R2).

It is known that the annealing process can reduce defect density [26]. Fig. 2 shows the results of the C_p-frequency after ICP-etched samples annealed at different temperatures in N_2 ambient for 30 min. We can also distinguish three types of interfacial states after 400 °C annealing process (N_2 400 samples). However, the capacitance at low frequency is reduced, and the plateau region is not so clear after 500 °C annealing process (N_2 500 samples). A smaller amount of the plateau region at low frequency for N_2 600 samples is observed, and the calculated LF-type interfacial states is $3.0 \times 10^{10}\,eV^{-1}\,cm^{-2}$. The HF-type interfacial states are reduced to $1.3 \times 10^{11}\,eV^{-1}\,cm^{-2}$ after 600 °C annealing process ($N_2$600 samples), which is quite near the value of the as-grown sample ($1.0 \times 10^{11}\,eV^{-1}\,cm^{-2}$, R1). The quantities of the LF- and MF-types interfacial states are less than that of the HF-type interfacial states for the N_2 600 sample. Thus, the N_2 annealing process is effective to remove both the LF- and MF-types interfacial states. Yet, the amount of HF-type interfacial states is slightly increased, and it can be observed as the annealing temperature is increased from 500 °C to 600 °C. The HF-type interfacial states become dominant for the ICP-etched sample after annealing in N_2 at 600 °C.

Fig. 3 shows the C_p-frequency results for an ICP-etched sample followed by 400 °C annealing process in H_2 ambient. The interface state capacitance at lower frequency is lower than that annealed in N_2 ambient. Thus, fewer LF-type interfacial states can be expected. In fact, the quantities of LF- and MF-types interfacial defects are both below those of HF-type interfacial states. The HF-type interfacial states increase with annealing temperature up to 400 °C,

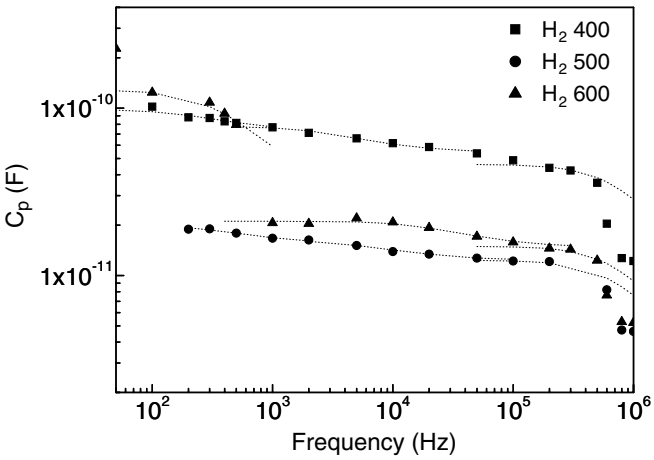

Fig. 3. Frequency dependence of C_p for the ICP-etched *n*-GaN sample after thermal annealing at 400 °C, 500 °C and 600 °C in H_2 ambient. The dot curves represent the fitting results of the experiment data.

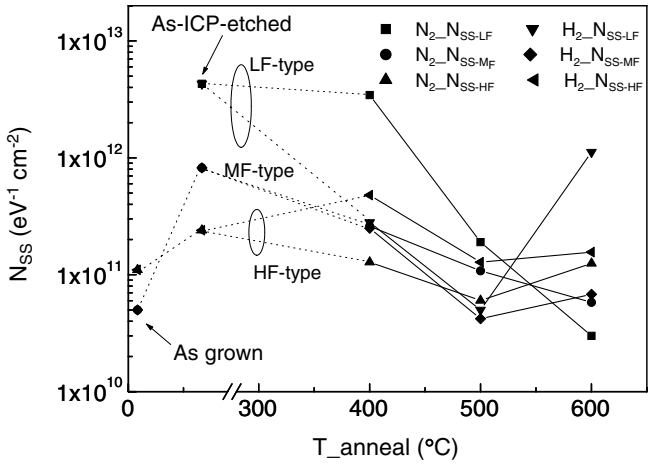

Fig. 4. Interfacial states density as a function of annealing temperature in N_2 ambient and H_2 ambient.

and decrease after annealing at 500 °C. The HF-type interfacial defects are dominant, and the density is around $4.8 \times 10^{11}\,eV^{-1}\,cm^{-2}$ for H_2 400 samples.

Both LF- and MF-types interfacial states decrease as the annealing temperature is increased up to 500 °C. However, as the temperature reaches 600 °C in H_2 ambient, a dramatic increase of the LF-type interfacial states. The interfacial state of both MF- and HF-type are slightly increased. In H_2 ambient, H_2 may diffuse and react chemically [27,28], so some hydrogen related defects may be formed and thus interfacial states are increased. The LF-type interfacial defects around $1.1 \times 10^{12}\,eV^{-1}\,cm^{-2}$ become dominant.

Fig. 4 shows the interfacial states density with annealing at different temperatures in N_2 and H_2 ambient respectively. In N_2 ambient, the ICP-induced LF-type and MF-type interfacial states decrease as the annealing temperature is increased from 400 °C to 600 °C. The HF-type interfacial states, around $1.0 \times 10^{11}\,eV^{-1}\,cm^{-2}$ for as-grown GaN, decrease slightly as the annealing temperature is increased from 400 °C to 500 °C, but increase as the temperature is increased from 500 °C to 600 °C. These embedded HF-type interfacial states cannot be reduced effectively via the annealing process in N_2 ambient.

While annealing in H_2 ambient, both LF-type and MF-type interfacial states decrease dramatically as the annealing temperature reached from 400 °C to 500 °C. Even the annealing temperature is as low as 400 °C in H_2 ambient, the LF-type interfacial states can be reduced to around one order of magnitude. In H_2 ambient, ICP-induced damage may be reduced to a lower level by H_2 diffusing and reacting chemically with the defects [26,29]. Thus, annealing under H_2 ambient is more effective to reduce the defects than under N_2 ambient. Yet, some hydrogen-related interfacial defects may arise in H_2 ambient as the temperature is increased from 500 °C to 600 °C. The LF-type interfacial states increase around one order of magnitude.

4. Conclusion

In conclusion the effects of thermally treated Schottky contact after ICP-etching were investigated. Due to ion bombardment, the ICP-etching process causes some damage. New interfacial state with low transition frequency around 300 Hz are found for an ICP-etched sample (R2). The overall interfacial states density of an as-grown sample (R1) and that of ICP-etched sample (R2) are around $10^{11}\,eV^{-1}\,cm^{-2}$ and $10^{12}\,eV^{-1}\,cm^{-2}$, respectively. After ICP-etching, three kinds of interfacial states were observed and characterized. The ICP-induced defects could be reduced by more than one order of magnitude after a subsequent annealing in N_2 ambient at 600 °C for 30 min or in H_2 ambient at 500 °C for 30 min. The H_2 ambient is more effective in removing these defects at temperature up to 500 °C. Additional defects may arise in H_2 ambient while the temperature is increased to 600 °C, whereas N_2 ambient shows good thermal stability with the annealing temperature up to 600 °C.

References

[1] Egawa T, Ishkawa H, Jimbo T, Umeno M. Recessed gate AlGaN/GaN modulation-doped field-effect transistors on sapphire. Appl Phys Lett 2000;76:121–3.
[2] Khan MA, Bhattarai A, Kuznia JN, Olson DT. High electron mobility transistor based on a GaN–$Al_xGa_{1-x}N$ heterojunction. Appl Phys Lett 1993;63:1214–5.
[3] Khan MA, Kuznia JN, Olson DT, Blasingame M, Bhattarai AR. Schottky barrier photodetector based on Mg-doped p-type GaN films. Appl Phys Lett 1993;63:2455–6.
[4] Nakamura S, Senoh M, Nagahama SI, Iwasa N, Yamada T, Matsushita T, et al. Room-temperature continuous-wave operation of InGaN multi-quantum-well-structure laser diodes with a long lifetime. Appl Phys Lett 1996;70:868–70.
[5] Cao XA, Cho H, Pearton SJ, Dang GT, Zhang AP, Ren F, et al. Depth and thermal stability of dry etch damage in GaN Schottky diodes. Appl Phys Lett 1999;75:232–4.
[6] Lee JM, Chang K-M, Kim SW, Huh C, Lee IH, Park SJ. Dry etch damage in n-type GaN and its recovery by treatment with an N_2 plasma. J Appl Phys 2000;87:7667–70.
[7] Nakaji M, Egawa T, Ishikawa H, Arulkumaran S, Jimbo T. Characteristics of BCl_3 Plasma-Etched GaN Schottky Diodes. Jpn J Appl Phys 2002;41:L493–5.
[8] Cho H, Vartuli CB, Abernathy CR, Donovan SM, Pearton SJ, Shul RJ, et al. Cl_2-based dry etching of the AlGaInN system in inductively coupled plasmas. Solid-State Electron 1998;42:2277–81.
[9] Kim HS, Yeom G-Y, Lee JW, Kim TI. A study of GaN etch mechanisms using inductively coupled Cl_2/Ar plasmas. Thin Solid Films 1999;341:180–3.
[10] Chyi JI, Lee CM, Chuo CC, Cao XA, Dang GT, Zhang AP, et al. Temperature dependence of GaN high breakdown voltage diode rectifiers. Solid-State Electron 2000;44:613–7.
[11] Zhang AP, Dang G, Ren F, Cao XA, Cho H, Lambers ES, et al. Cl_2/Ar High-Density-Plasma Damage in GaN Schottky Diodes. J Electrochem Soc 2000;147:719–22.
[12] Lee JM, Kim SW, Park SJ. Dry Etching of GaN/InGaN Multiquantum Wells Using Inductively Coupled $Cl_2/CH_4/H_2$/Ar Plasma. J Electrochem Soc 2001;148:G254–7.
[13] Cheung R, Withanage S, Reeves RJ, Brown SA, Ben-Yaacov I, Kirchner C, et al. Reactive ion etch-induced effects on the near-band edge luminescence in GaN. Appl Phys Lett 1999;74:3185–7.

[14] Achouche M, Clei A, Harmand JC. Characterization of electrical damage induced by CH_4/H_2 reactive ion etching of molecular beam epitaxial InAlAs. J Vac Sci Technol 1996;B14:2555–66.
[15] Anand S, Subramanian S, Arora BM. Use of low-frequency capacitance in deep level transient spectroscopy measurements to reduce series resistance effects. J Appl Phys 1992;72:3535–8.
[16] Schmeits M, Nguyen ND, Germain M. Competition between deep impurity and dopant behavior of Mg in GaN Schottky diodes. J Appl Phys 2001;89:1890–7.
[17] Kar S, Dahlke WE. Interface states in MOS structures with 20–40 Å thick SiO_2 films on nondegenerate Si. Solid-State Electron 1972; 15:221–37.
[18] Deneuville A. Characterization of the interface states at a Ag/Si interface from capacitance measurements. J Appl Phys 1974;45 :3079–84.
[19] Singh A. Characterization of interface states at Ni/*n*CdF_2 Schottky barrier type diodes and the effect of CdF_2 surface preparation. Solid-State Electron 1985;28:223–32.
[20] Singh A, Cova P, Masut RA. Energy density distribution of interface states in Au Schottky contacts to epitaxial $In_{0.21}Ga_{0.79}As$:Zn layers grown on GaAs by metalorganic vapor phase epitaxy. J Appl Phys 1993;74:6714–9.
[21] Tseng Hsun-Hua, Wu Ching-Yuan. A simple technique for measuring the interface-states density of the Schottky barrier diodes using the current-voltage characteristics. J Appl Phys 1987;61:299–304.
[22] Chen Zhi, Park Dae-Gyu, Stengal Francke, Noor Mohammad S, Morkoc Hadis. Metal-insulator-semiconductor structures on p-type GaAs with low interface states density. Appl Phys Lett 1996;69:230–2.
[23] Roberts GI, Crowell CR. Capacitance Energy Level Spectroscopy of Deep-Lying Semiconductor Impurities Using Schottky Barriers. J Appl Phys 1970;41:1767–76.
[24] Beguwala M, Crowell CR. Characterization of multiple deep level systems in semiconductor junctions by admittance measurements. Solid-State Electron 1974;17:203–14.
[25] Fernandez-Canque HL, Allison J, Thompson MJ. The capacitance of rf sputtered hydrogenated amorphous silicon Schottky barrier diodes. J Appl Phys 1983;54:7025–33.
[26] Cao XA, Zhang AP, Dang GT, Cho H, Ren F, Pearton SJ, et al. Inductively coupled plasma damage in GaN Schottky diodes. J Vac Sci Technol 1999;B17:1540–4.
[27] Kim J, Ren F, Gila BP, Abernathu CR, Pearton SJ. Reversible barrier height changes in hydrogen-sensitive Pd/GaN and Pt/GaN diodes. Appl Phys Lett 2003;82:739–41.
[28] Sawada Masakazu, Sawada Takayuki, Yamagata Yuji, Imai Kazuaki, Kimura Hisahito, Yoshino Masaki, et al. Electrical characterization of *n*-GaN Schottky and PCVD-SiO_2/*n*-GaN interfaces. J Cryst Growth 1998;189–190:706–10.
[29] Deal BE, MacKenna EL, Castro PL. Characteristics of fast surface states associated with SiO_2–Si and Si_3N_4–SiO_2–Si structures. J Electrochem Soc 1969;116:997–1005.